# Learning from the Lund plane

Epiphany 2020, Krakow, 10 January 2020

Frédéric Dreyer

UNIVERSITY OF OXFORD

based on arXiv:1807.04758, arXiv:1903.09644 and arXiv:1909.01359

with Stefano Carrazza, Gavin Salam & Gregory Soyez

# Boosted objects at the LHC

- At LHC energies, EW-scale particles (W/Z/t. . . ) are often produced with $p_t \gg m$, leading to collimated decays.
- Hadronic decay products are thus often reconstructed into single jets.

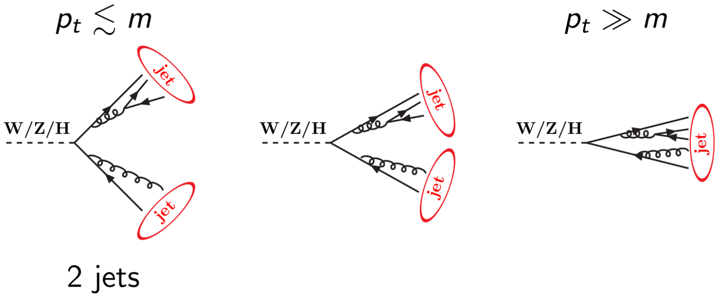


[Figure by G. Soyez]

- At LHC energies, EW-scale particles (W/Z/t...) are often produced with $p_t \gg m$, leading to collimated decays.
- Hadronic decay products are thus often reconstructed into single jets.

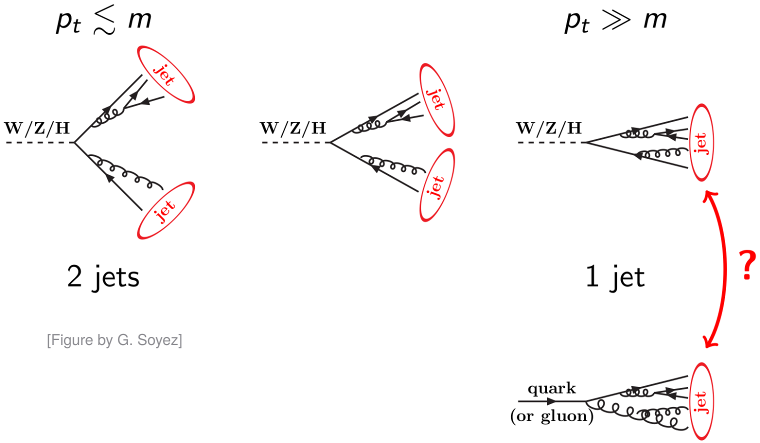


[Figure by G. Soyez]

# Boosted objects at the LHC

- Many techniques developed to identify hard structure of a jet based on radiation patterns.
- In principle, simplest way to identify these boosted objects is by looking at the mass of the jet.

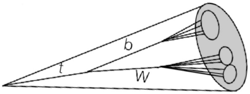


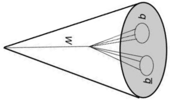

# Boosted objects at the LHC

- Many techniques developed to identify hard structure of a jet based on radiation patterns.
- In principle, simplest way to identify these boosted objects is by looking at the mass of the jet.
- But jet mass distribution is highly distorted by QCD radiation and pileup.

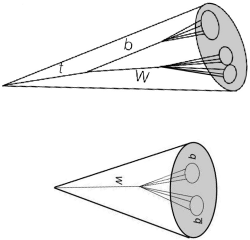


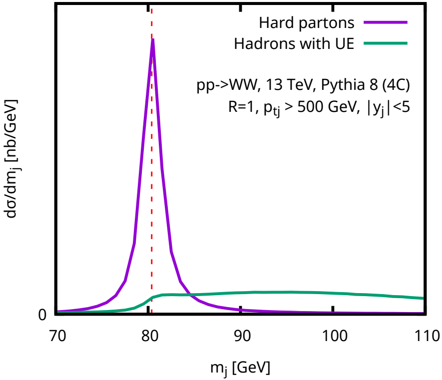

# Identifying boosted objects

Two main approaches to study boosted decays:

1. Manually constructing substructure observables that help distinguish between different origins of jets.
2. Apply machine learning models trained on large input images or observable basis.

**Aim of this talk:** new approaches bridging some of the gap between these two techniques.

# Jet grooming: (Recursive) Soft Drop / mMDT

- Mass peak can be partly reconstructed by removing unassociated soft wide-angle radiation (grooming).
- Recurse through clustering tree and remove soft branch if

$$\frac{\min(p_{t,1}, p_{t,2})}{p_{t,1} + p_{t,2}} < z_{\text{cut}} \left(\frac{\Delta R_{12}}{R_0}\right)^{\beta}$$

W jet

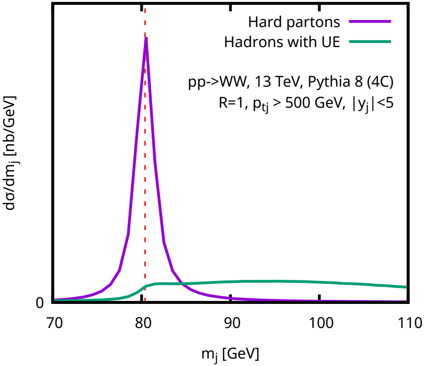


[Dasgupta, Fregoso, Marzani, Salam JHEP 1309 (2013) 029]
[Larkoski, Marzani, Soyez, Thaler JHEP 1405 (2014) 146]
[FD, Necib, Soyez, Thaler JHEP 1806 (2018) 093]

- Mass peak can be partly reconstructed by removing unassociated soft wide-angle radiation (grooming).
- Recurse through clustering tree and remove soft branch if

$$\frac{\min(p_{t,1}, p_{t,2})}{p_{t,1}+p_{t,2}} < z_{\text{cut}} \left(\frac{\Delta R_{12}}{R_0}\right)^{\beta}$$

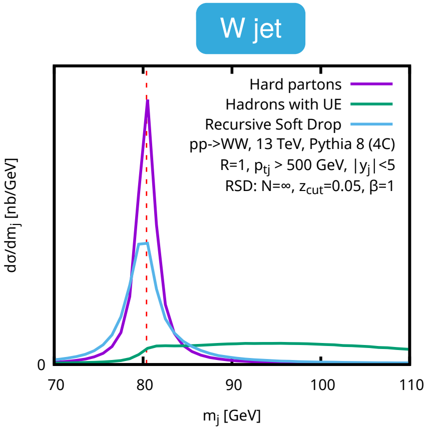


[Dasgupta, Fregoso, Marzani, Salam JHEP 1309 (2013) 029]
[Larkoski, Marzani, Soyez, Thaler JHEP 1405 (2014) 146]
[FD, Necib, Soyez, Thaler JHEP 1806 (2018) 093]

- Variety of observables have been constructed to probe the hard substructure of a jet ($V/H/t$ decay lead to jets with multiple hard cores).
- Radiation patterns of colourless objects ($W/Z/H$) differs from quark or gluon jets.
- Efficient discriminators can be obtained e.g. from ratio of $N$-subjettiness or energy correlation functions.

[Thaler, Van Tilburg JHEP 1103 (2011) 015]
[Larkoski, Salam, Thaler JHEP 1306 (2013) 108]
[Larkoski, Moult, Neill JHEP 1412 (2014) 009]

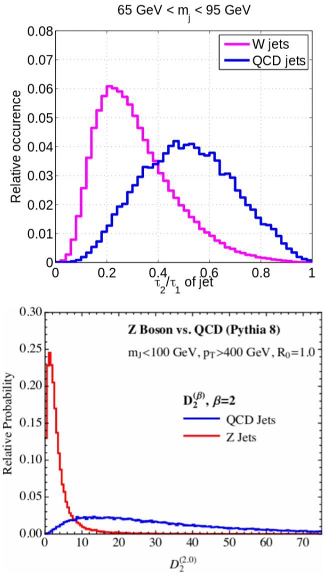

# Applying Machine Learning in Jet Physics

Recent wave of results in applications of ML algorithms to jet physics.

Classification problems have been tackled through several orthogonal approaches

- Convolutional Neural Networks used on representation of jet as image
- Recurrent Neural Networks used on jet clustering tree.
- Linear combination or dense network applied to an observable basis (e.g. $N$-subjettiness ratios, energy flow polynomials)

# Beyond classification problems

- Classification problems are one of the easiest application of ML, but by far not the only one!
- Many promising applications of ML methods for:
  - fast simulations using unsupervised generative models
    [Paganini, de Oliveira, Nachman PRL 120 (2018) 042003]
  - regression tasks such as pile-up subtraction
    [Komiske, Metodiev, Nachman, Schwartz JHEP 1712 (2017) 051]
  - anomaly detection for new physics
    [Collins, Howe, Nachman PRL 121 (2018) 241803]
  - distance metric of collider events
    [Komiske, Metodiev, Thaler arXiv:1902.02346]
  - etc ...
- See ML4Jets conference taking place at NYU next week!

# THE LUND PLANE

# Lund diagrams

- Lund diagrams in the $(\ln z\theta, \ln\theta)$ plane are a very useful way of representing emissions.
- Different kinematic regimes are clearly separated, used to illustrate branching phase space in parton shower Monte Carlo simulations and in perturbative QCD resummations.
- Soft-collinear emissions are emitted uniformly in the Lund plane

$$dw^2 \propto \alpha_s \frac{dz}{z}\frac{d\theta}{\theta}$$

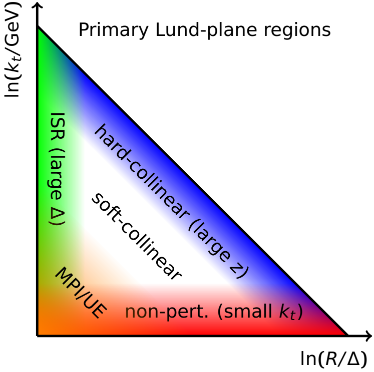

Features such as mass, angle and momentum can easily be read from a Lund diagram.

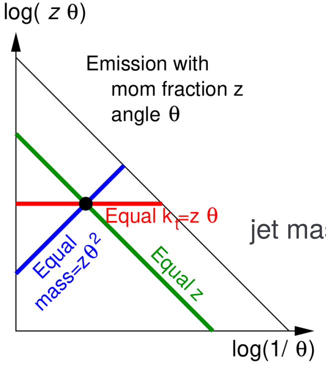


jet mass $\equiv \frac{m^2}{p_t^2 R^2} \approx z_1 \theta_1^2$

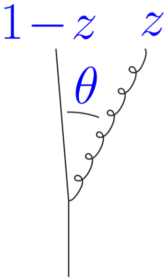

# Lund diagrams for substructure

Substructure algorithms can often also be interpreted as cuts in the Lund plane.

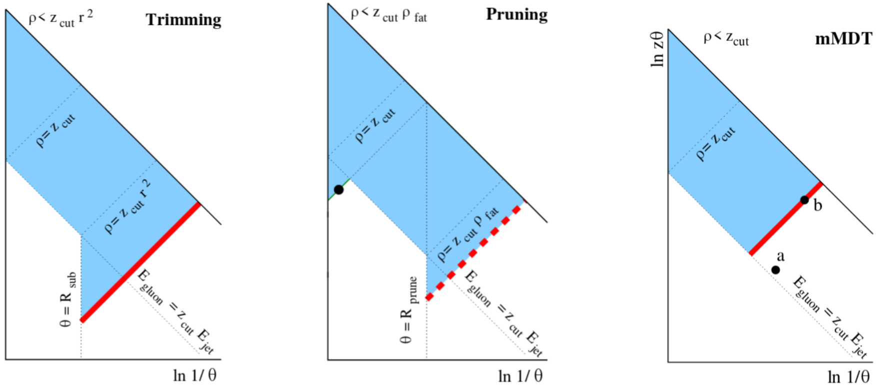


[Dasgupta, Fregoso, Marzani, Salam JHEP 1309 (2013) 029]

# Studying jets in the Lund plane

Lund diagrams can provide a useful approach to study a range of jet-related questions

- First-principle calculations of Lund-plane variables.
- Constrain MC generators, in the perturbative and non-perturbative regions.
- Brings many soft-drop related observables into a single framework.
- Impact of medium interactions in heavy-ion collisions.
- Boosted object tagging using Machine Learning methods.

We will use this representation as a novel way to characterise radiation patterns in a jet, and study the application of recent ML tools to this picture.

# Lund plane representation

To create a Lund plane representation of a jet, recluster a jet $j$ with the Cambridge/Aachen algorithm then decluster the jet following the hardest branch.

1. Undo the last clustering step, defining two subjets $j_1, j_2$ ordered in $p_t$.
2. Save the kinematics of the current declustering
$$\Delta \equiv (y_1 - y_2)^2 + (\phi_1 - \phi_2)^2, \quad k_t \equiv p_{t2}\Delta,$$
$$m^2 \equiv (p_1 + p_2)^2, \quad z \equiv \frac{p_{t2}}{p_{t1}+p_{t2}}, \quad \psi \equiv \tan^{-1}\frac{y_2-y_1}{\phi_2-\phi_1}.$$
3. Define $j = j_1$ and iterate until $j$ is a single particle.

# Lund plane representation

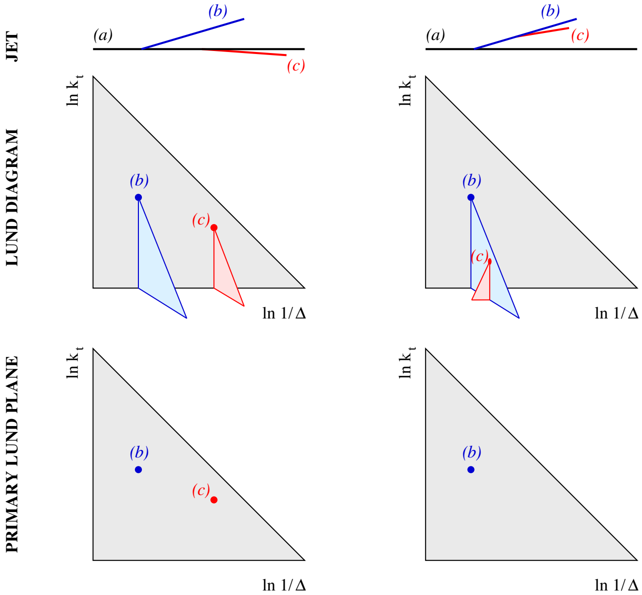

- Each jet has an image associated with its primary declustering.
- For a C/A jet, Lund plane is filled left to right as we progress through declusterings of hardest branch.
- Additional information such as azimuthal angle $\psi$ can be attached to each point.

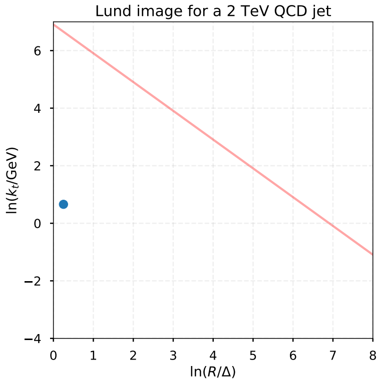


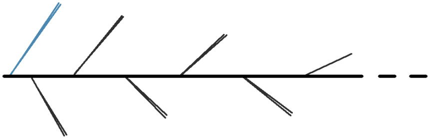

# Lund representation of a jet

- Each jet has an image associated with its primary declustering.
- For a C/A jet, Lund plane is filled left to right as we progress through declusterings of hardest branch.
- Additional information such as azimuthal angle $\psi$ can be attached to each point.

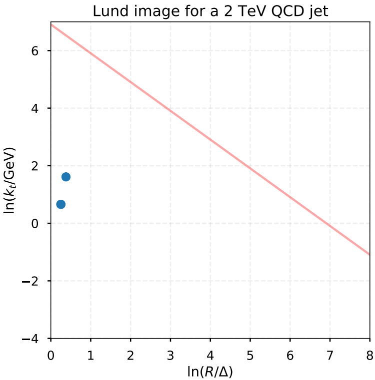


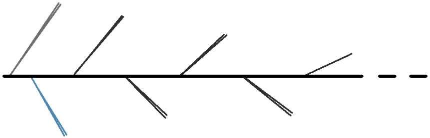

# Lund representation of a jet

- Each jet has an image associated with its primary declustering.
- For a C/A jet, Lund plane is filled left to right as we progress through declusterings of hardest branch.
- Additional information such as azimuthal angle $\psi$ can be attached to each point.

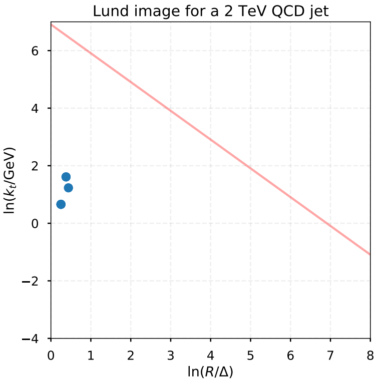


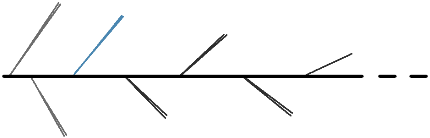

# Lund representation of a jet

- Each jet has an image associated with its primary declustering.
- For a C/A jet, Lund plane is filled left to right as we progress through declusterings of hardest branch.
- Additional information such as azimuthal angle $\psi$ can be attached to each point.

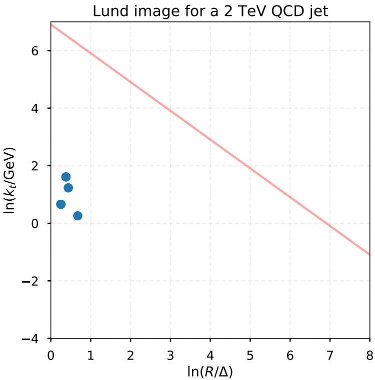


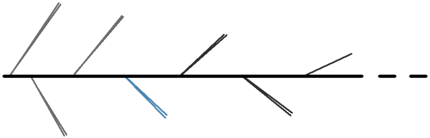

- Each jet has an image associated with its primary declustering.
- For a C/A jet, Lund plane is filled left to right as we progress through declusterings of hardest branch.
- Additional information such as azimuthal angle $\psi$ can be attached to each point.

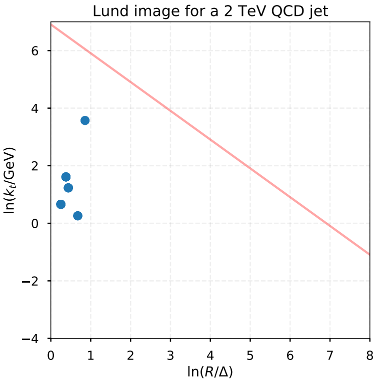


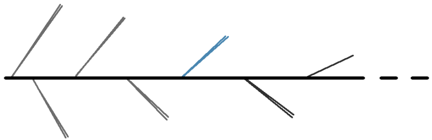

# Lund representation of a jet

- Each jet has an image associated with its primary declustering.
- For a C/A jet, Lund plane is filled left to right as we progress through declusterings of hardest branch.
- Additional information such as azimuthal angle $\psi$ can be attached to each point.

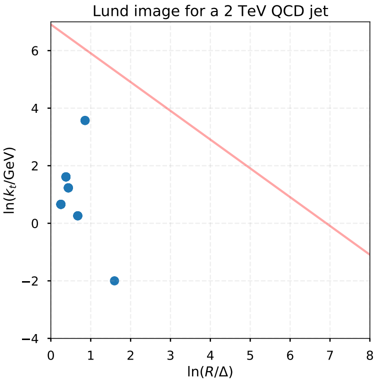


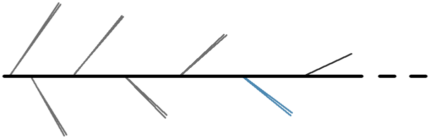

# Lund representation of a jet

- Each jet has an image associated with its primary declustering.
- For a C/A jet, Lund plane is filled left to right as we progress through declusterings of hardest branch.
- Additional information such as azimuthal angle $\psi$ can be attached to each point.

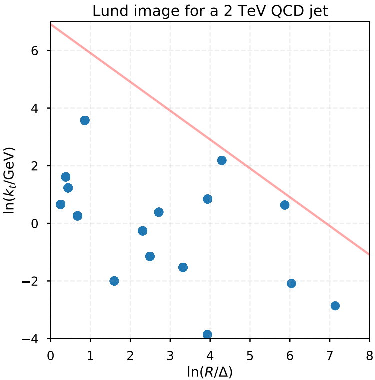


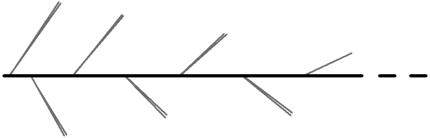

# Jets as Lund images

Average over declusterings of hardest branch for 2 TeV QCD jets.

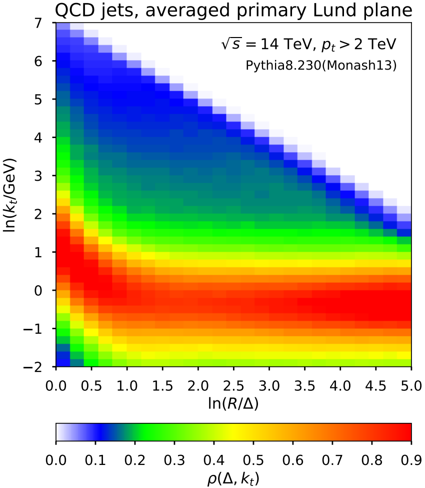


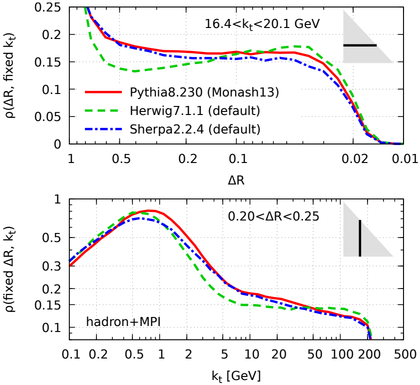


$$\rho \sim 2C\frac{\alpha_s(k_t)}{\pi}$$

# Jets as Lund images

Average over declusterings of hardest branch for 2 TeV QCD jets.

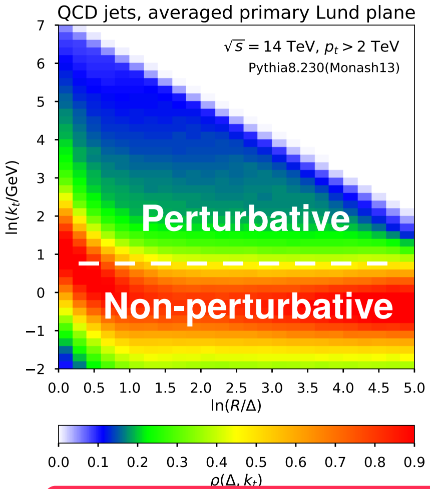


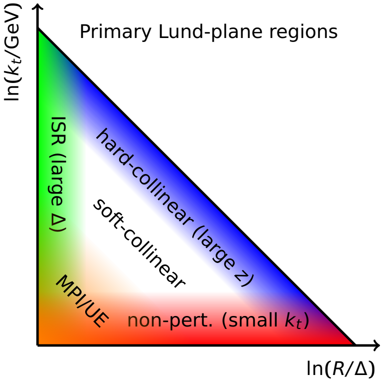


Non-perturbative region clearly separated from perturbative one.

## Jets as Lund images

Average over declusterings of hardest branch for 2 TeV QCD jets.

hadron+MPI⟶ parton

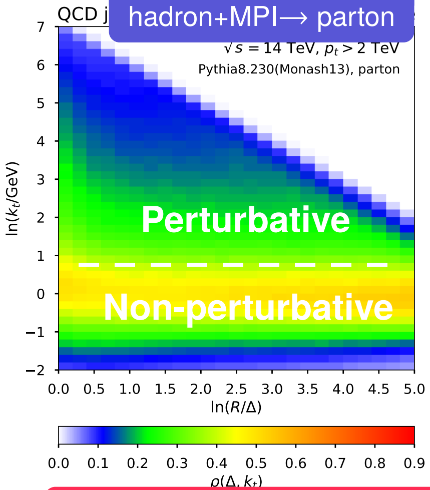


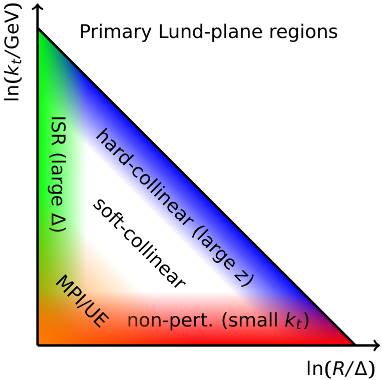


Non-perturbative region clearly separated from perturbative one.

# Analytic study of the Lund plane

To leading order in perturbative QCD and for $\Delta \ll 1$, one expects for a quark initiated jet

$$\rho \simeq \frac{\alpha_s(k_t)C_F}{\pi}\bar{z}\left(p_{gq}(\bar{z}) + p_{gq}(1-\bar{z})\right), \quad \bar{z} = \frac{k_t}{p_{t,\text{jet}}\Delta}$$

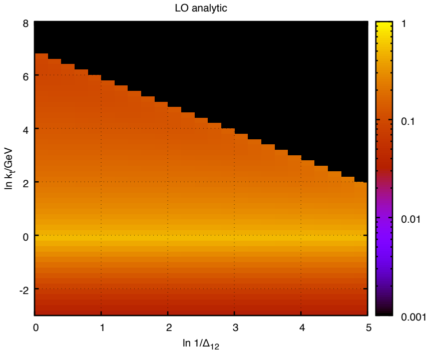


- Lund plane can be calculated analytically.
- Calculation is systematically improvable.

# Analytic study of the Lund plane

To leading order in perturbative QCD and for $\Delta \ll 1$, one expects for a quark initiated jet

$$\rho \simeq \frac{\alpha_s(k_t) C_F}{\pi} \bar{z} \left( p_{gq}(\bar{z}) + p_{gq}(1-\bar{z}) \right), \quad \bar{z} = \frac{k_t}{p_{t,\text{jet}} \Delta}$$

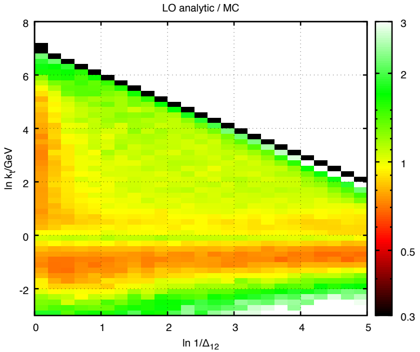


- Lund plane can be calculated analytically.
- Calculation is systematically improvable.

To leading order in perturbative QCD and for $\Delta \ll 1$, one expects for a quark initiated jet

$$\rho \simeq \frac{\alpha_s(k_t)C_F}{\pi}\bar{z}\left(p_{gq}(\bar{z}) + p_{gq}(1-\bar{z})\right), \quad \bar{z} = \frac{k_t}{p_{t,\mathrm{jet}}\Delta}$$

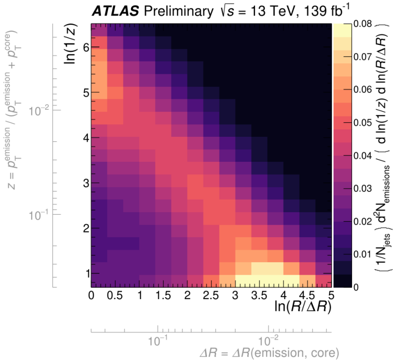


- Lund plane can be calculated analytically.
- Calculation is systematically improvable.
- Can be compared to data.

# Declustering other jet-algorithm sequences

- Choice of C/A algorithm to create clustering sequence related to physical properties and associated to higher-order perturbative structures
- anti-$k_t$ or $k_t$ algorithms result in double logarithmic enhancements

$$\bar{\rho}_2^{(\text{anti-}k_t)}(\Delta,\kappa) \simeq +8C_F\, C_A \ln^2 \frac{\Delta}{\kappa} \qquad\qquad \bar{\rho}_2^{(k_t)}(\Delta,\kappa) \simeq -4C_F^2 \ln^2 \frac{\Delta}{\kappa}$$

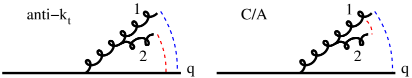


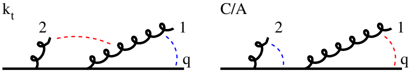

# Declustering other jet-algorithm sequences

- Choice of C/A algorithm to create clustering sequence related to physical properties and associated to higher-order perturbative structures
- anti-$k_t$ or $k_t$ algorithms result in double logarithmic enhancements

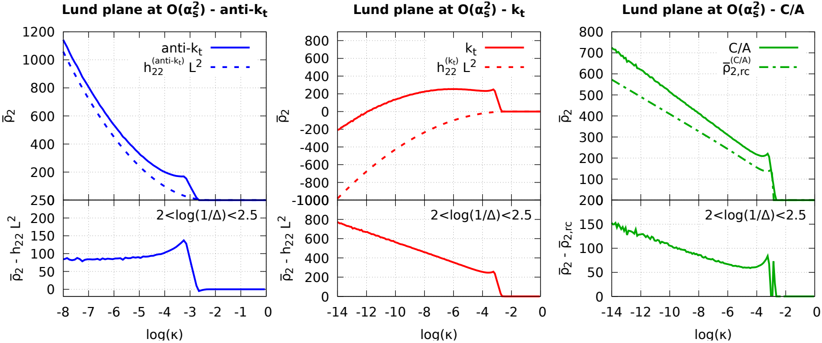

- Hard splittings clearly visible, along the diagonal line with jet mass $m = m_W$.

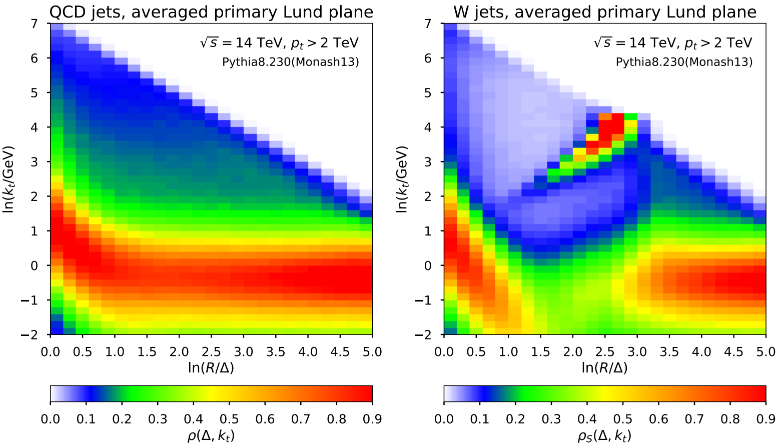

# APPLICATION TO BOOSTED OBJECT TAGGING

# Tagging jets in the Lund Plane

We will now investigate the potential of the Lund plane for boosted-object identification.

Two different approaches:

- A log-likelihood function constructed from a leading emission and non-leading emissions in the primary plane.
- Use the Lund plane as input for a variety of Machine Learning methods.

As a concrete example, we will take dijet, $WW$ and $t\bar{t}$ events.

- LL approach already provides substantial improvement over best-performing substructure observable.
- LSTM network substantially improves on results obtained with other methods.
- Large gain in performance, particularly at higher efficiencies.

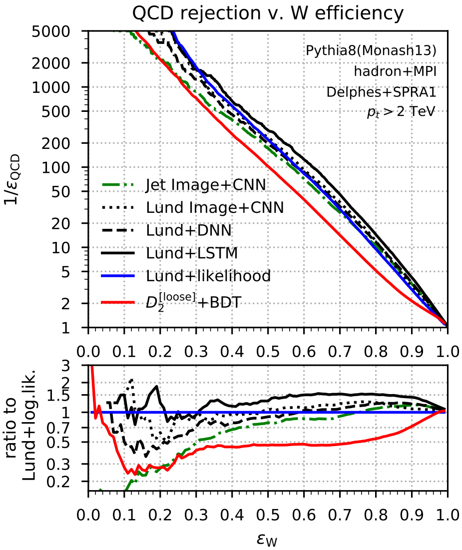

# Boosted top tagging

- For top tagging primary declustering sequence doesn't capture the full substructure information.
- Can achieve large gains in performance by taking into account the full tree.
- Dynamic Graph CNN based methods perform particularly well.

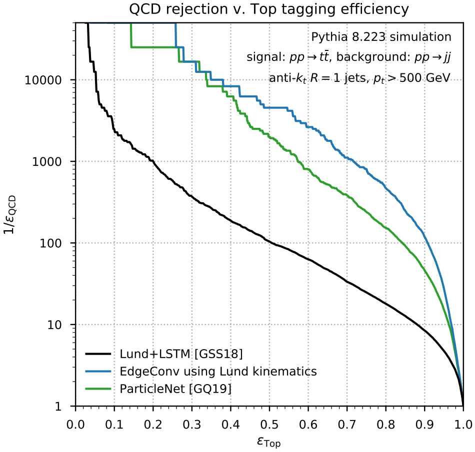

# Sensitivity to non-perturbative effects

- Performance compared to resilience to MPI and hadronisation corrections.
- Vary cut on $k_t$, which reduces sensitivity to the non-perturbative region.

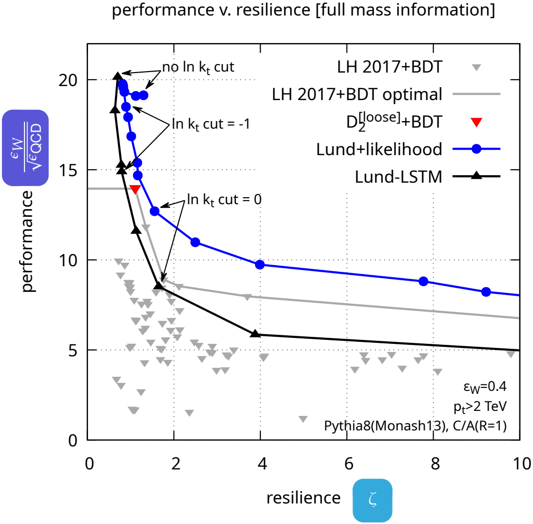


$$\Delta\epsilon = \epsilon - \epsilon'$$

$$\zeta = \left( \frac{\Delta\epsilon_S^2}{\langle\epsilon\rangle_S^2} + \frac{\Delta\epsilon_B^2}{\langle\epsilon\rangle_B^2} \right)^{-\frac{1}{2}}$$

(c.f. arXiv:1803.07977)

$$\langle\epsilon\rangle = \frac{1}{2}(\epsilon + \epsilon')$$

- Lund-likelihood performs well even at high resilience.
- ML approach reaches very good performance but is not particularly resilient to NP effects.

# LUND IMAGES USING GANS

# Learning to generate Lund images

- Images are combined in small batches of $32$, each pixel value interpreted as the probability of being switched on.
- Preprocess images with rescaling and ZCA whitening.

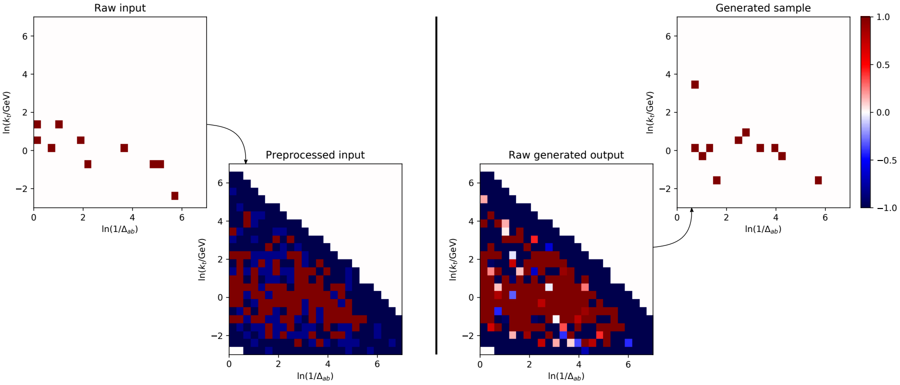

# Learning to generate Lund images

- Images are combined in small batches of $32$, each pixel value interpreted as the probability of being switched on.
- Preprocess images with rescaling and ZCA whitening.

We consider three generative models

- Two Generative Adversarial Network architectures (LSGAN and WGANGP), constructed from generator $G$ and discriminator $D$ which compete against each other through a value function $V(G,D)$

$$\min_G \max_D V(D,G) = \mathbb{E}_{x\sim p_{\text{data}}}[\log D(x)] + \mathbb{E}_{z\sim p_z(z)}[\log(1-D(G(z)))]\,,$$

- and a latent variable VAE model, which uses a probabilistic encoder $q_\phi(z|x)$, and decoder $p_\theta(x|z)$ to map from prior $p_\theta(z)$. The algorithm learns the marginal lilelihood of the data in this generative process

$$\mathcal{L}(\theta,\phi) = \mathbb{E}_{q_\phi(z|x)}[\log p_\theta(x|z)] - \beta D_{\text{KL}}(q_\phi(z|x)||p(z))\,,$$

To avoid posterior collapse of VAE, we use KL annealing.

# Lund images from GANs

- The LSGAN provides the most stable results.
- Differences between models can be studied using slices of the Lund plane or derived observables.

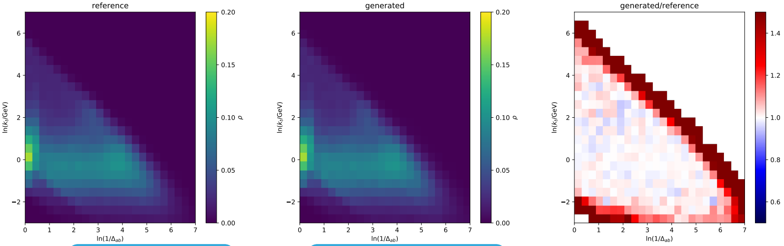


Fixed $k_t$ slice

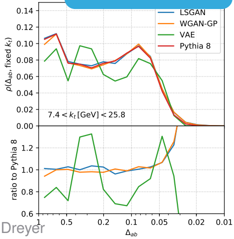


Fixed $\Delta_{ab}$ slice

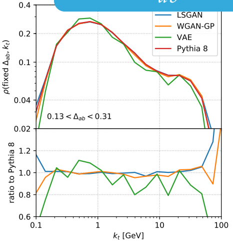


Soft Drop multiplicity

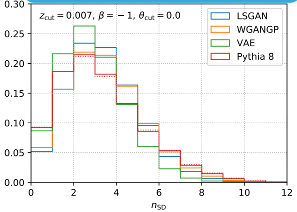

# Cycle-consistent adversarial networks

- CycleGAN learns unpaired image-to-image mapping functions $G : X \to Y$ and $F : Y \to X$ between two domains $X$ and $Y$.
- Forward cycle consistency $x \in X \to G(x) \to F(G(x)) \approx x$ and backward cycle consistency $y \in Y \to F(y) \to G(F(y)) \approx y$, achieved through cycle consistency loss.
- Full objective includes also adversarial losses to both mapping functions.

$$\mathcal{L}(G,F,D_X,D_Y) = \mathcal{L}_{\text{GAN}}(G,D_Y,X,Y) + \mathcal{L}_{\text{GAN}}(F,D_X,Y,X) + \lambda\,\mathcal{L}_{\text{cyc}}(G,F)\,.$$

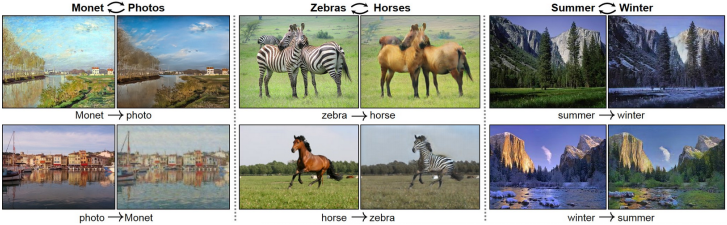

# Reinterpreting events with CycleGANs

- Use CycleGAN to transform between two different domains of Lund images, e.g.
  - $W$ jet $\leftrightarrow$ QCD jet
  - parton-level simulation $\leftrightarrow$ detector-level simulation
- Apply trained network to transform Lund images event-by-event by cycling through domains.
- Transformed events in good agreement with true sample.

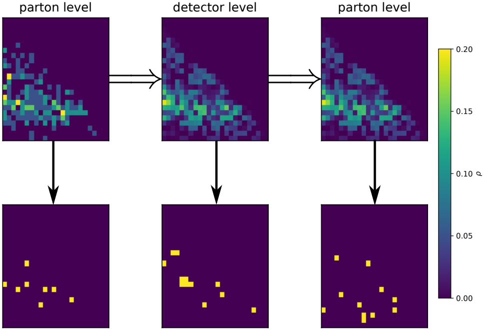

# Reinterpreting events with CycleGANs

- Use CycleGAN to transform between two different domains of Lund images, e.g.
  - $W$ jet $\leftrightarrow$ QCD jet
  - parton-level simulation $\leftrightarrow$ detector-level simulation
- Apply trained network to transform Lund images event-by-event by cycling through domains.
- Transformed events in good agreement with true sample.

$W \leftrightarrow$ QCD

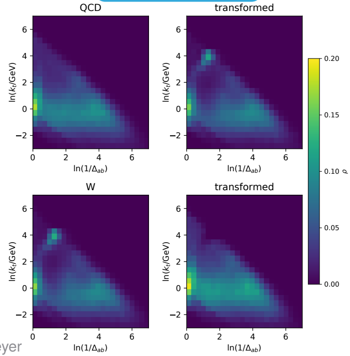


parton $\leftrightarrow$ detector

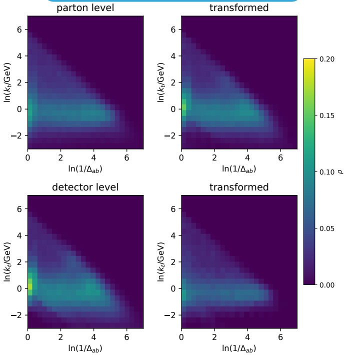

# CONCLUSIONS

# Conclusions

- Discussed a new way to study and exploit radiation patterns in a jet using the Lund plane.
- Lund kinematics can be used as inputs for $W$ tagging with a range of methods:
  - Log-likelihood function.
  - Convolutional neural networks.
  - Recurrent and dense neural networks.
  - Graph convolutional networks.

  Simple LL approach already provides strong performance, sometimes even matching the one obtained with recent ML methods.
- Provides a framework for promising application of generative models and reinforcement learning.

Wide range of experimental and theoretical opportunities brought by studying Lund diagrams for jets. A **rich topic** for **further exploration**.

# BACKUP SLIDES

# Log-likelihood use of Lund Plane

Log-likelihood approach takes two inputs:

- First one obtained from the "leading" emission, defined as first emision satisfying $z > 0.025$ ($\sim$ mMDT tagger).

$$\mathcal{L}_\ell(m,z) = \ln\left(\frac{1}{N_S}\frac{dN_S}{dmdz}\bigg/\frac{1}{N_B}\frac{dN_B}{dmdz}\right)$$

- The second one which brings sensitivity to non-leading emissions.

$$\mathcal{L}_{n\ell}(\Delta, k_t; \Delta^{(\ell)}) = \ln\left(\rho_S^{(n\ell)}/\rho_B^{(n\ell)}\right)$$

Overall log-likelihood signal-background discriminator for a given jet is then given by

$$\mathcal{L}_{\text{tot}} = \mathcal{L}_\ell(m^{(\ell)}, z^{(\ell)}) + \sum_{i\neq\ell}\mathcal{L}_{n\ell}(\Delta^{(i)}, k_t^{(i)}; \Delta^{(\ell)}) + \mathcal{N}(\Delta^{(\ell)})$$

# Tagging with LL method

- Compare the LL approach in specific mass-bin with equivalent results from the Les Houches 2017 report (arXiv:1803.07977).
- Substantial improvement over best-performing substructure observable.